Asian Journal of Nanoscience and Materials 5 (2022) 36-47

Asian Journal of Nanoscience and Materials

Journal homepage: www.ajnanomat.com

Original Research Aarticle

Investigation and synthesis of Fe doped Al_2O_3 nanoparticles by Co-precipitation and sol gel methods

Abolfazl Khodadadi[a,*], Mohammad Rahim Talebtash[b,*]

[a] *Department of Physics, Tehran North Branch, Islamic Azad University, Tehran, Iran*

[b] *Department of Engineering, Shahriar Branch, Islamic Azad University, Shahriar, Iran*

ARTICLE INFORMATION

Received: 5 November 2021
Received in revised: 21 December 2021
Accepted: 24 December 2021
Available online: 24 January 2022

DOI: 10.26655/AJNANOMAT.2022.1.4

KEYWORDS

Fe-Al_2O_3
NPs
Dopant

ABSTRACT

This study doped alumina with iron impurities by co-precipitation and sol-gel methods compared with pure alumina. Precursors of aluminum and iron metal salts employ the surfactant and new stabilizers used for synthesizing samples. Several analysewere performed on different properties of the synthesized samples and the effect of iron impurities on them. The presence of different phases was confirmed in the XRD spectrum of nanoparticles made by co-precipitate method. As the percentage of impurities increases, the unstable and intermediate phases decrease and eventually tend to the stable phase of α-alumina, the resulting hexagonal structure is obtained. The FESEM spectra of samples synthesized by both methods showed that a decrease in particle size occurs with an increase in the percentage of impurities. TEM analysis of nanoparticles with 5% impurity shows the shape of the particles as quasi-spherical, about agglomerate. It is the reason for removing the stabilizing agent in the high-temperature heating process. Also, increasing the intermolecular gravitation force, the particles stick together in a lump. UV-DSR analysis showed that with increasing impurity percentage, the energy band gap decreases and the absorption wavelength λ_{edge} increases. In samples fabricated in both methods, the value of E_g obtained is close to each other. The VSM spectrum showed that ferromagnetic properties occur when iron enters alumina sites.

Corresponding author, email: A.Khodadadi@iau-tnb.ac.ir (A. Khodadadi).
Tel.: +98 912 212 9136.

Graphical Abstract

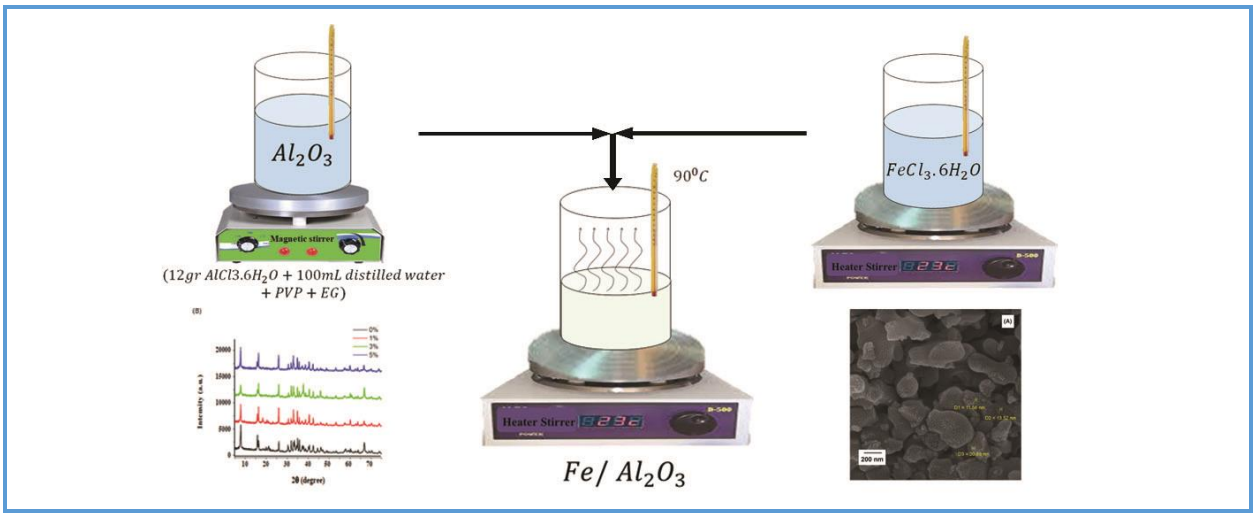

Introduction

In recent decade, metal oxide semiconductors have been used in different areas of industry [1–9]. Alumina (Al_2O_3) is used as a high heat conductivity insulator. Due to high adsorption, alumina is used as a catalyst [10–14]. By increasing the surface-to-volume ratio, the properties of this nanomaterial are changed. The energy band gap of alumina is 6-8 eV. It has several crystalline phases, which the most stable phase is α by hexagonal crystal structure and formed in 1200 °C. It is used as a catalyst protector in ceramic and composites [15]. The other phases of alumina such as $\gamma, \eta, \kappa, \chi, \beta, \theta, \delta$ are thermodynamically unstable and by increasing impurity and heat changes to the α phase [16–21]. The primary agent of instability is the configuration of its atoms; empty sites in octahedral and tetrahedral γ-alumina [21]. According to the kind of impurity and the size of the particles, the γ-alumina changes to the intermediate phases and finally to the stable α phase [15]. When the transition elements are doped to alumina, their physical properties improve [22–27]. Fe has a high surface density, and its ionic radius is close to that of aluminum. So, the magnetic and optical properties of aluminaalumina's magnetic and optical properties improved by Fe dopant. By adding Fe^{3+} ions, impurities enter the alumina. This changes the magnetic properties to ferromagnetic behavior [28–30]. And the energy band gap reduced by adding Fe^{3+} ions. [31]. Both physical and chemical methods can do the synthesis of NPs. Each one has its characteristics because of particle growth and uniformity [32, 33]. Chemical methods include sol-gel, co-precipitation, hydrothermal, sonochemistry, emulsion, and electrochemistry methods [34–38]. In this research, pure alumina and Fe doped alumina with different dopants are synthesis by the sol-gel and co-precipitation methods. Various analyzVarious analyzVarious analyzes studied the properties of doped nanoparticles studied the properties of doped nanoparticles studied the properties of doped nanoparticles.

Experimental

Materials and methods

In this study for synthesis alumina, pure alumina and Iron salts such as $Fe_2(SO_4).9H_2O$, $9Al_2(SO_4)3.9H_2O$, $AlCl_3.6H_2O$, PVP, PEG, ethanol,

Iron mitral salt were used. The structural study was performed by X-ray diffraction (XRD), and data with 2θ in the angle range (0 °-80 °) with the type X-Pert Pro MPD, Cu-Kα (λ = 1.54060 A °) was recorded. The transmission of the optical spectrum in the infrared spectrum (FTIR) was performed by a spectrum RXI infrared Fourier transform spectrometer manufactured by Perkin Elmer. The appearance and average size of nanoparticles were determined by transmission electron microscopy (TEM) with Zeiss EM-900 model (80 kv). To determine the absorption wavelength and the optical energy gap of the samples, SHIMADZU (UV-1800) reflectance spectroscopy was used. Also, to study nanoparticles' microscopic structure and uniformity, a field scanning electron microscope (FESEM) with TE-SCAN's MIRA3 device has been used. The magnetic behavior of the samples was evaluated by a vibrating sample magnetometer (VSM) with Lake Shore 7400 model at room temperature.

First method

By sol-gel method Al_2O_3 and Fe/Al_2O_3 Np_s were synthesize. The precursore $AlCl_3$ and $FeCl_3$ were used for this method. First, for synthase of the alumina, 6.5 g of $AlCl_3.6H_2O$ dissolved in 50 mL of distilled water. A magnetic stirrer was used for stirring the solution at room temperature for 15 minutes. In another container, 1 g of PVP was dissolved in 12.5 mL distilled water. After that 6 mL ethanol was added to the solution at 60 °C The temperature was increased to 80 °C. In this temperature, to remove impurities, 5 mL PVP was added to the solution from the sample. Then 6 mL of EG added to the solution. The process of heating was continued until the temperature of the solution was received to 90 °C, it was starting to dry. Throughout the experiment, PH of the solution was 3. Finally, the product obtained was washed with ethanol and pure water several times to get a pure product.

To synthesize the Fe/Al_2O_3, 6.75 g of $FeCl_3.6H_2O$ was dissolved in 50 mL of pure water. The solution 0.5 mol/L was obtained. Then it was added to the alumina solution at different *Fe* percentage 2%, 3%, and 5%, and the rest of the process was followed as the pure sample.

The resulting powder was calcined at 1000 °C for 4 hours. Then the final product was prepared for various spectra, such as X-ray diffractometer (XRD), emission scanning electron microscope (FESEM), transmission electron microscopy (TEM), Fourier-transform infrared spectroscopy (FTIR), diffuse reflection spectroscopy (DRS), and VSM.

This analysis proved that the doped sample has magnetic properties.

The second method

Al_2O_3 and Fe/Al_2O_3 NPs with the precursors of $Al_2(SO_4)_3.9H_2O$ and $Fe_2(SO_4)_3.9H_2O$ were synthesized using co-precipitation procedure. First, the particularspecific amount of aluminum iron nitrate salt was dissolved in 50 mL of pure water. Then, the solution was heated. In 80 °C, the alkaline agent NaOH was slowly added to it, then the temperature was raised to 90 °C.

For the synthesis o*f* Fe/Al_2O_3 nanoparticles with 2%, 3%, and 5%, a certain amount of iron nitrate salt was dissolved in 50 mL of distilled water. Dopped samples with different percentages were calcined at 1400 °C for 5 h. Finally, the powder samples were analyzed, and different analyzerdifferent analyzers investigated the effect of doped iron in alumina investigated the effect of doped iron in alumina.

Results and Discussion

XRD analysis

Figure 1**a** shows the XRD analysis of Al_2O_3 and Fe/Al_2O_3 samples with different percentages (2%, 3%, 5%) in sol-gel method. According to these spectra, after doping alumina by iron, structure of the alumina (hexagonal structure), did not change. In this case, the Fe^{+3} ion replaced by Al^{+3} ion in Al_2O_3 matrix. This replacement caused a slight change in the network constants. There was a difference of 0.06 $\dot{A}$ between the ion radius of iron and alumina. The replacement of Fe^{+3} ion in alumina crystal makes this difference and changes the grain boundaries.

Particle size based on impurity 1.3 and 5% were determined 28.1, 30.2 and 32.5 nm respectively. It represents that by increasing the amount of iron impurity, the nanoparticles' size decreases.

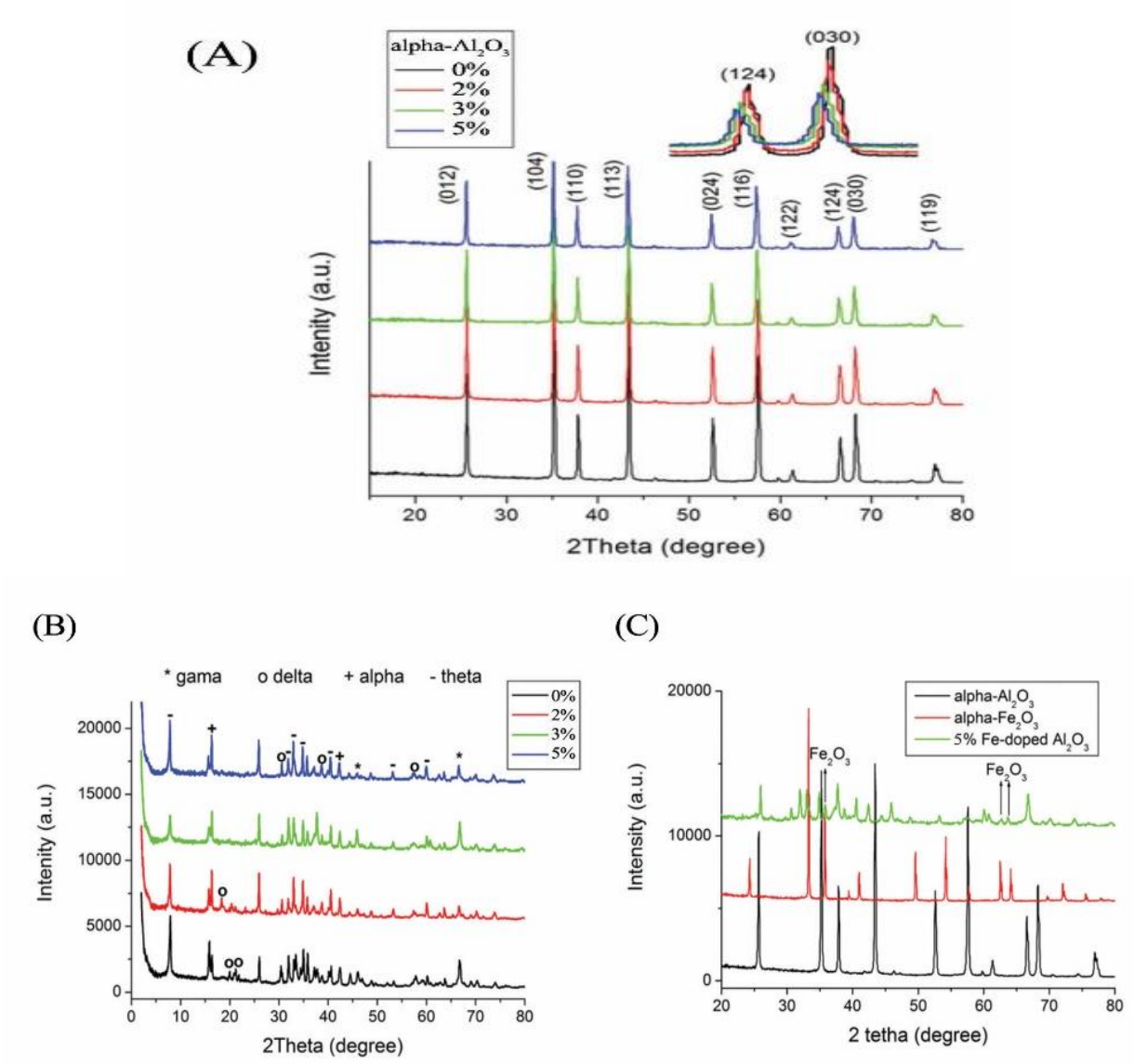

Figure 1. a) XRD Spectra of sol gel method, b) XRD spectra of co-precipitation method, and c) XRD peaks of the α-Fe_2O_3, α-Al_2O_3 and 5% Fe-doped alumina sample

Figure 1**b** shows the XRD analysis of samples in co-precipitation method. As iron enters the alumina matrix during the synthesis process, it affects the γ-Al_2O_3 phase. The structure of alumina is affected by different percentages of doped iron and replaces Fe^{3+} with Al^{3+}. So, the XRD spectrum of doped samples shifts. In the samples, other phases of alumina were expected to form. In the sample spectrum with 5% impurity, the α-Al_2O_3 phase is visible. This phenomenon indicates that a certain amount of Fe^{3+} ions have been replaced in the γ-Al_2O_3 lattice and has prevented crystal growth. Therefore, the size of the doped crystal is smaller than that of the pure sample. The shifts in the spectrum confirm the existence of different alumina phases in the synthesized sample. In this case, the size of the crystal cannot be determined through the Scherrer relation [39].

For sample by 5% impurity, for the crystallization rate of the γ, δ and Θ phases, the peak levels 17%, 25%, and 55% were determined, respectively. The peaks generated at angles 35.12º , 48.8º , 62.5º and 63.7º indicate the presence of α-Fe_2O_3 phases (JCPDS Card No. 29-0063) (Figure 1**b**). These peaks show that Fe^{+3} is located in the empty places of the alumina lattice and for a certain amount of iron impurities embedded in the γ-Al_2O_3, the presence of α-Fe_2O_3 phase is obtained in the γ-Al_2O_3 crystal lattice phase.

FESEM analysis

FESEM analysis was performed to determine the morphology and size of the NPs synthesized. According this analysis (Figure 2), when Fe doping percentage increased, the size of the NPs decreased. So that the most suitable condition of uniform distribution in the impurity state of 3% iron was obtained using the co-precipitation method. Also, the smallest particle size of 30 nm for 5% impurity was obtained in sol-gel method.

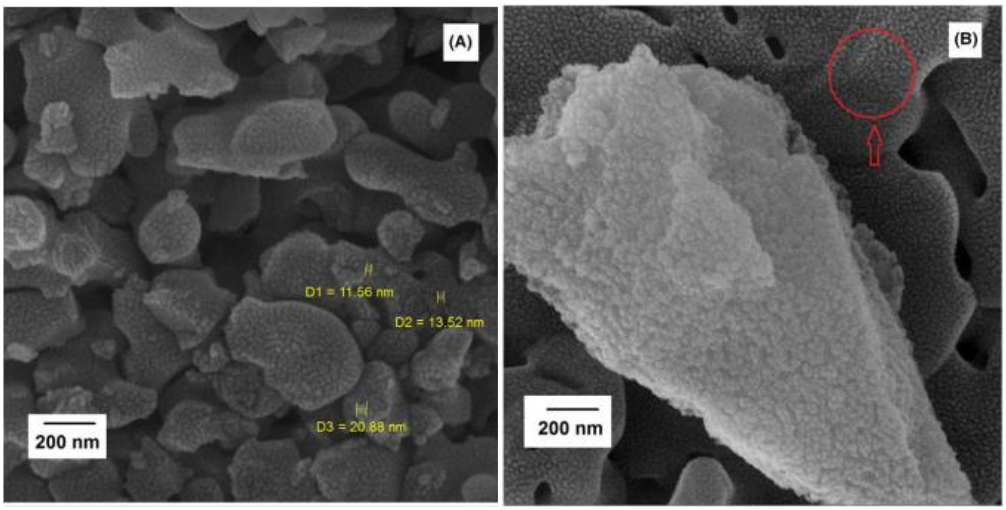

Figure 2. Field-emission scanning electron microscope images of a) pure Al_2O_3, b) 3 %mol, Fe-doped Al_2O_3

Figure 3 shows the morphology of Fe-doped Al_2O_3 NPs with different dopants that it was performed by the coprecipitation method. Coating SEM samples with only 1 nm of Au increases the signal-to-noise ratio dramatically, resulting in crisp and clear images. As the figure illustrates, when iron impurities are added, the size of the NPs decreases while their morphology increases. When the size decreases, the interatomic and molecular forces increase.

Subsequently, NPs tend to be closer to each other, resulting in their aggregation. The aggregation is resolved when the EG stabilizer is added to the sample [40–44]. The average calculated mean value for NPs with 57 nm in size and impure NPs with 2%, 3%, and 5% impurities is 51 nm, 49 nm, and 46 nm, respectively.

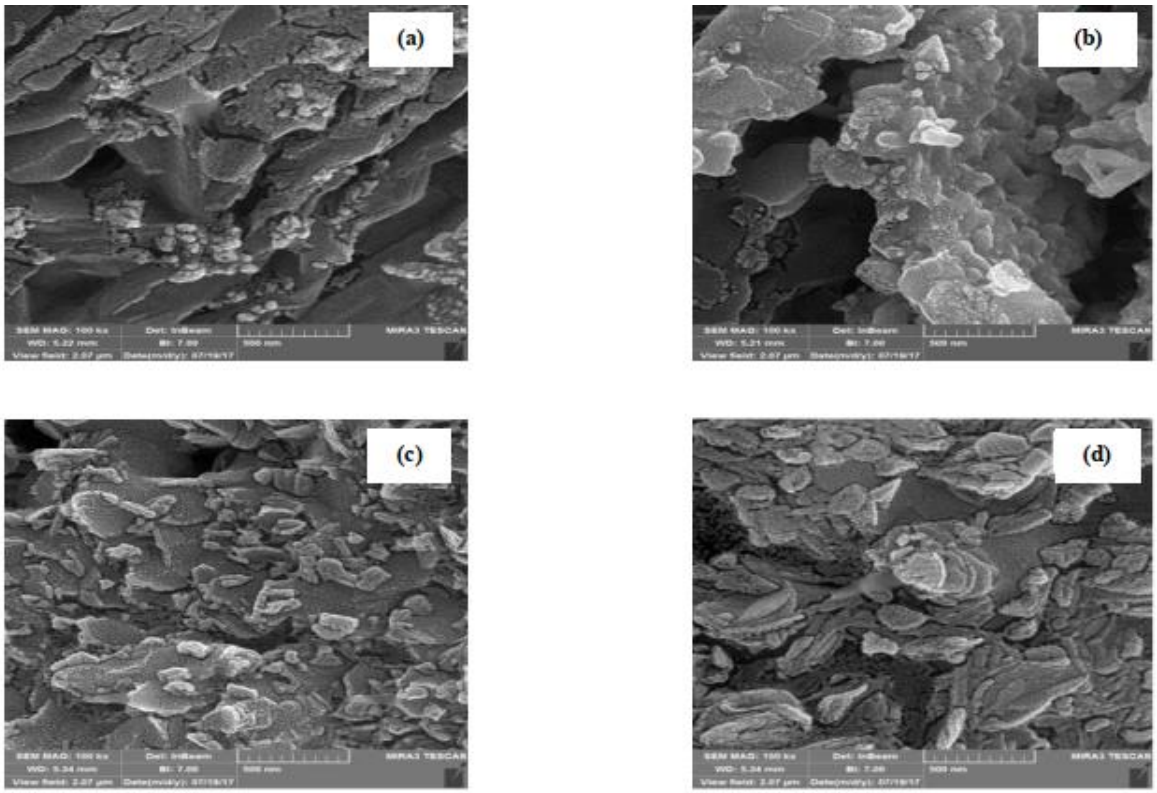

Figure 3. FESEM images of a) pure alumina, b) 2%, c) 3% and d) 5% Fe-doped Al_2O_3

FTIR analysis

FTIR analysis was used to determine the functional group and vibration band. Figure 4**a** shows the transmission rate of samples in the co-precipitation method. The strong absorption peak in the wavelength of 3085 cm^{-1} was associated with the O–H group from water molecules independent gel powder.

The absorption peak created in the wavelength of 2360 cm^{-1} related to the C–H vibration band. As it can be seen, the peak in the frequency of 450 cm^{-1} related to hematite (α-Fe_2O_3) which confirms the results of XRD analysis.

Figure 4**b** shows a sample's FTIR spectrum with a 5% impurity in thesol-gel method. The absorption peak created at wavelength 2349 cm^{-1} related to the C–H vibrational bond. The peak created in the wavenumber 1561 cm^{-1} related to the C=C tensile vibration bond. Also, the peak of intense absorption at wave 584 cm^{-1} related to the Al–O vibration bond. The two absorption peaks at 845 cm^{-1} and 631 cm^{-1} related to the vibration of AlO_4 at the tetrahedral site and AlO_6 at the octahedral site of the alumina.

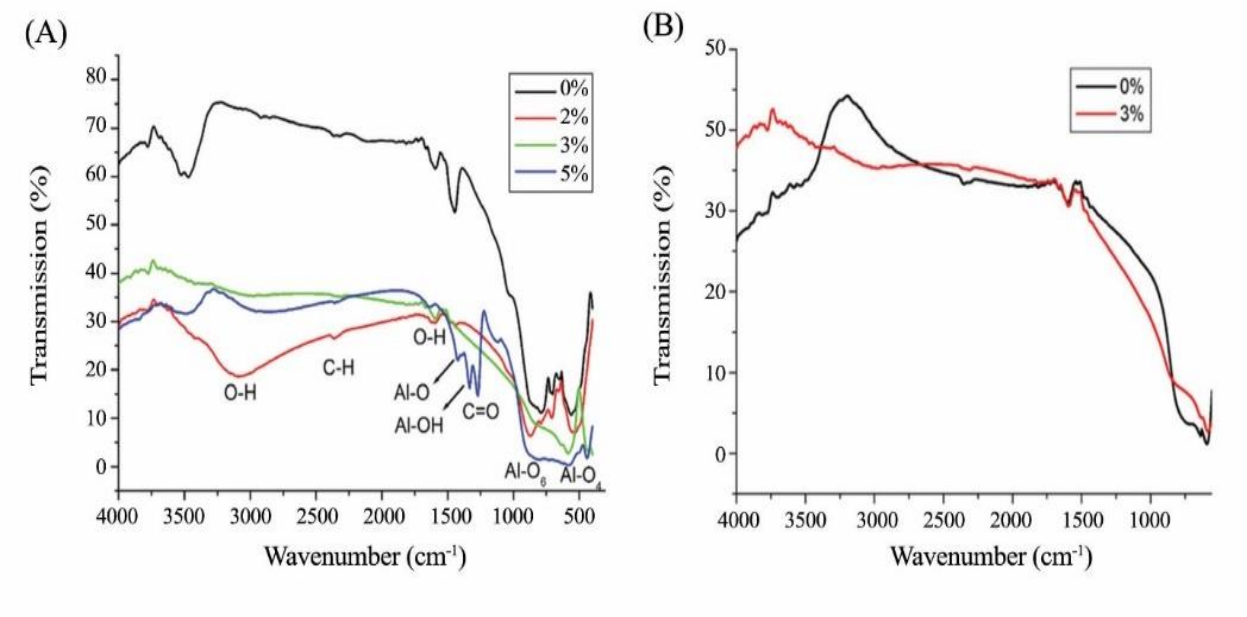

Figure 4. Fourier-transform infrared spectroscopy spectrum of the pure and Fe-doped Al_2O_3 nanocomposites, by a) co-precipitation method b) solgel method

TEM analysis

TEM analysis was conducted to determine the precise size and appearance of the nanoparticles,. Figure 5 reveals the TEM analysis of Al_2O_3 NPs with 5% dopant (by sol-gel method). As can be seen, the shape of the NPs is quasi-spherical and is stuck together to some extent; this is due to the removal of PVP and EG stabilizers after heating at 1000 °C. Indeed, with the elimination of the stabilizers, the interatomic and intermolecular forces of attraction of the NPs increased, causing their agglomeration. Furthermore, the curve of the function of the size distribution of the NPs showed their mean size to be in the region of 27.70 nm and a standard deviation of 0.99 nm.

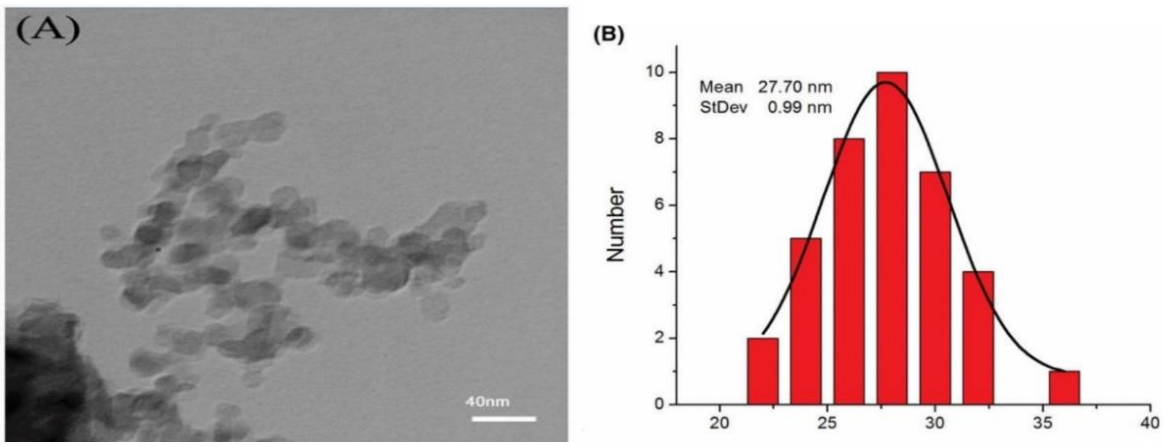

Figure 5. Transmission electron microscopy image of 5 mol% Fe-doped Al_2O_3 samples

TEM analyses of the pure and doped samples were used to determine the exact size and appearance of the NPs (for co-precipitation method). As shown in Figure 6, NPs doped with 5% impurity are synthesized in the form of aggregation, and their average size is about 45 nm. The low Fe content led to this typical grain morphology for the undoped alumina. The TEM showed grains of different sizes and iron oxide species presumably covering the surface of the grains, which is per XRD data. According to the TEM results, the NPs have a quasi-spherical shape aggregated together due to the removal of EG stabilizer after being heated at 1000 °C. Indeed, by eradicating the stabilizers, the atomic force of the NPs grows via producing the aggregates [42, 45].

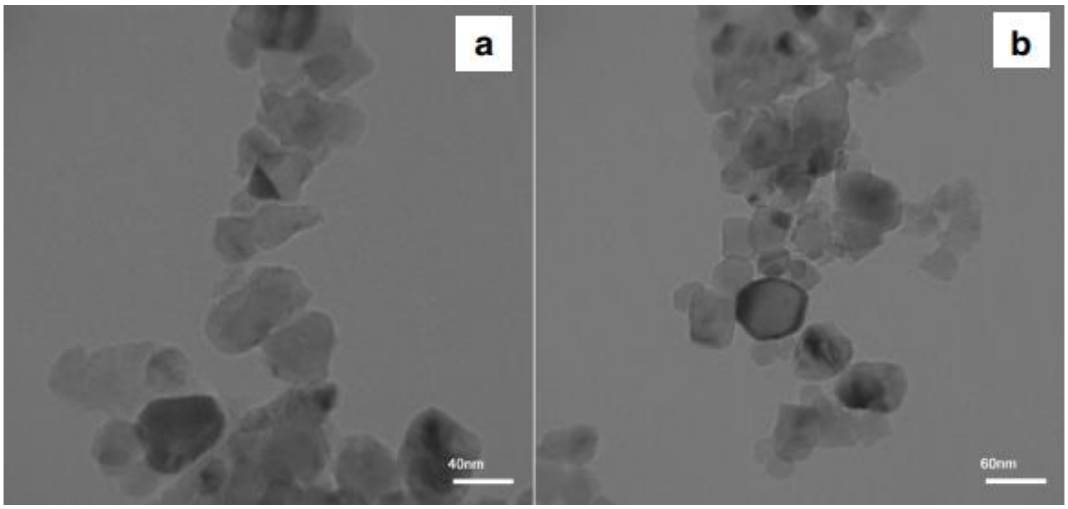

Figure 6. Transmission electron microscopy (TEM) image of a undoped and b 5% Fe-doped Al_2O_3 samples annealed at 1000 °C

UV-DRS optical study

UV radiation analysis was used to determine the samples' absorption wavelength and band gap energy. The results are shown in Figure 7. By increasing amount of doped iron impurities of sample fabricated by co-precipitation method, the absorption wavelength increases from 285 nm for pure particles to 365 nm for nanoparticles with a 5% impurity. Therefore, the reduction of the energy bandgap also occurs. The energy band gap was plotted on the energy curve $(F(R)hv)^2$ using the tauc function. $F(R)$ is a Kubelka-Munk function [44, 45]. The results show that the energy gap of 4.01, 3.70, 3.60, and 3.53 is obtained for pure and impure samples of 2%, 3% and 5% impurity, respectively.

The sample results made by the sol-gel method show that the energy gap of 4.0, 3.87, 3.62, and 3.42 is obtained for pure and impure samples of 2%, 3%, and 5% impurity, respectively.

The energy gap calculated in this method has been significantly reduced compared to the published reports (Eg = 6ev). The reason for this decrease is the sp-d interactions of the energy band. The d electrons in the impurity band and the band electrons in at the bottom of the alumina conduction band.

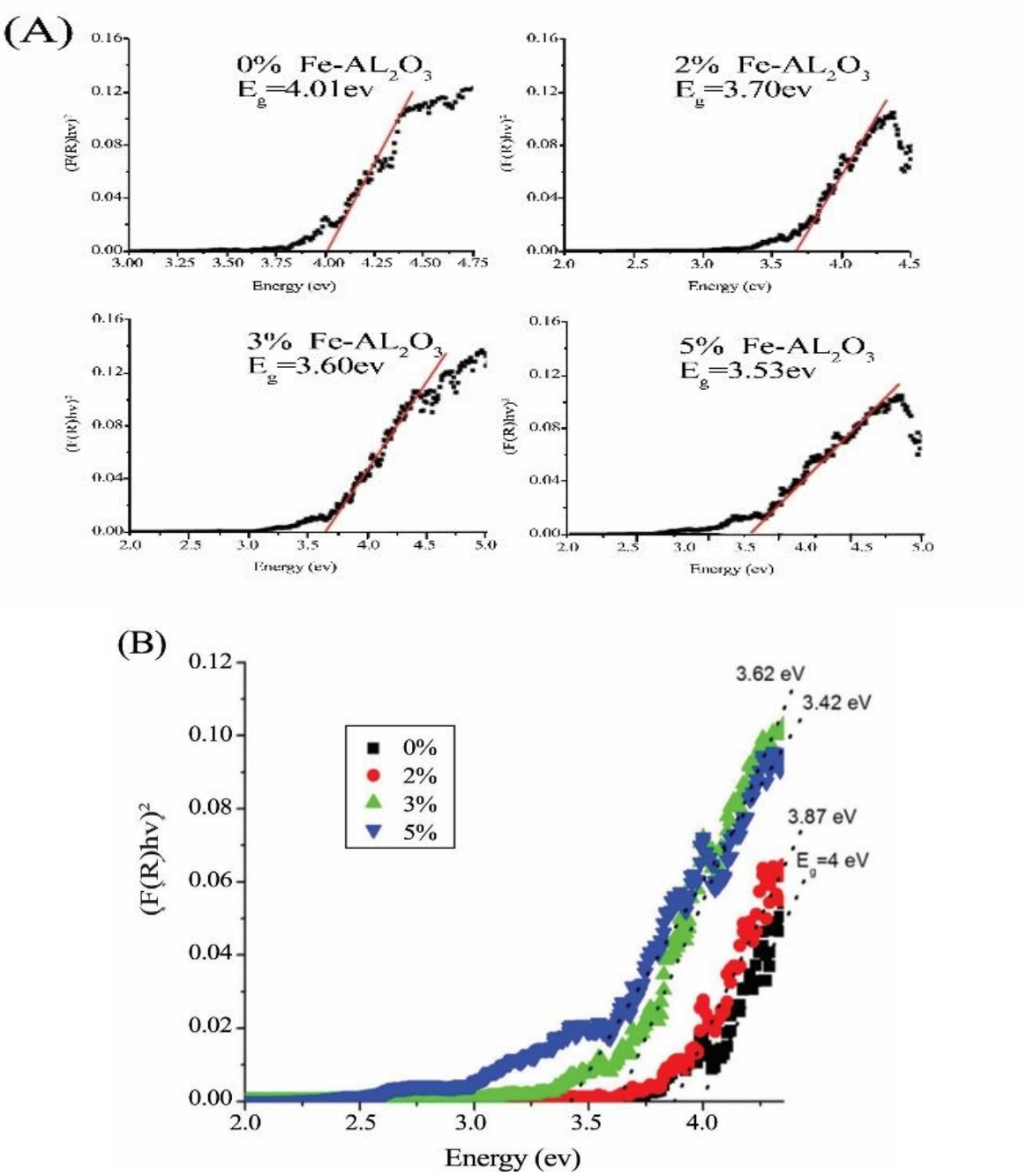

Figure 7. Tauc plot of $[F(R)hv]^{1/2}$ vs E (hv) energy of the Fe/Al_2O_3 NPs with different Fe dopants, a) co-precipitation method b) solgel method

Magnetic properties

Pure alumina is a diamagnetic. The entry of Fe impurities causes a $d-d$ bond between Fe and Al. As a result, a magnetic bond is formed between the atoms. In this case, the magnetic dipoles are oriented, and the magnetic property is strengthened. Therefore, the doped sample with impurities has ferromagnetic properties at room temperature.

VSM analysis was used to determine the magnetic behavior of the sample. In co-precipitation method, the Saturation

magnetization (M_s) of 5% doped sample was 0.136 emu / g and Coercivity field (H_c) was 139.4 G (Figure 8**a**).

SimilarlySimilarly, the VSM spectra of the nanoparticle sample with 3% impurity by sol gel method were performed. M_s and H_c of 5% doped sample was 0.140 emu / g 128.4 , respectably (Figure 8**a**). The results comparing to other studies increased significantly. [48–49].

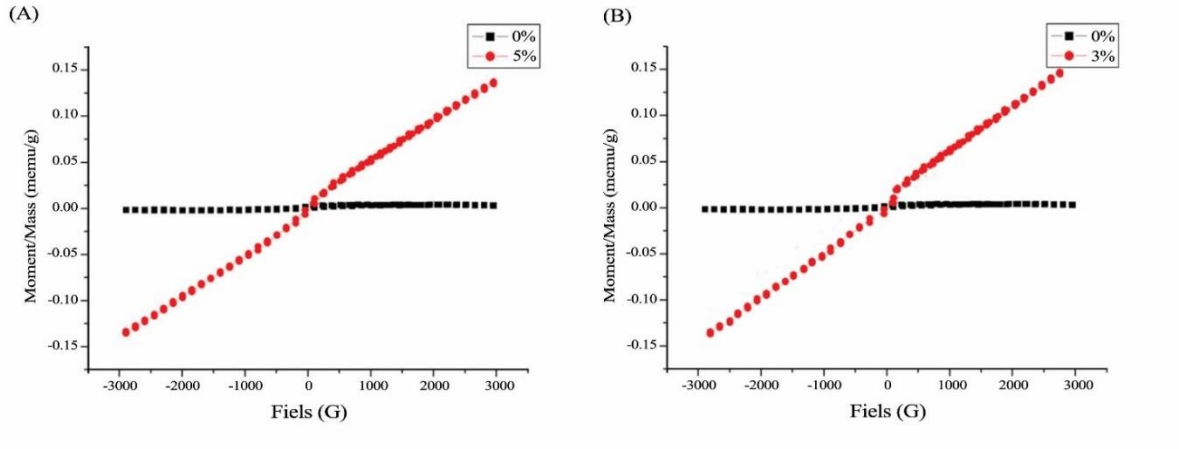

Figure 8. VSM analysis, (M-H) curve of undoped and Fe dopants, a) in co-precipitation method b) in solgel method

Conclusions

Pure Al_2O_3 nanoparticles were fabricated with iron-alumina composite nanoparticles using two methods: sol-gel and precipitation. Aluminum and iron salts, surfactants, and desired stabilizers were used. The XRD results showed a hexagonal structure for the samples synthesized by sol-gel method. In the sample synthesized by the co-precipitation method, impurities caused different phases in the structure of crystalline nanoparticles. For a certain amount of iron impurities, the structure remains unchanged. In both methods, it was observed that the size of nanocrystals decreases. FTIR results indicate an increase in the Al–OH vibrational band with increasing Fe impurities. UV-DRS spectrum analysis shows a reduction in the energy bandgap with increasing impurities and red transfer. The results of VSM analysis show ferromagnetic behavior in doped samples and an increase in ferromagnetic properties of samples by increasing the percentage of impurities.

Disclosure Statement

No potential conflict of interest was reported by the authors.

Orcid

Abolfazl Khodadadi 0000-0001-6145-0361

Mohammad Rahim Talebtash 0000-0002-2007-9866

References

[1]. Dastpak M., Farahmandjou M., Firoozabadi, T.P. *J. Supercond. Nov. Magn.,* 2016, **29**:2925

[2]. Farahmandjou M., Soflaee F. *Chin. J. Phys.,* 2015, **53**:080801

[3]. Jurablu S., Farahmandjou M., Firoozabadi T.P. *J. Theoretical. Appl. Phys.,* 2015, **9**:261

[4]. Farahmandjou M., Soflaee F. *Phys.Chem. Res.*, 2015, **3**:193

[5]. Zarinkamar M., Farahmandjou M., Firoozabadi T.P. *J.Nanostruct.*, 2016, **6**:116
[6]. Farahmandjou M. *J. Phys.Res.,* 2016, **16**:1
[7]. Farahmandjou M., Ramazani M. *Phys. Chem.Res.,* 2015, **3**:293
[8]. Shadrokh S., Farahmandjou M., Firozabadi T.P. *Phys. Chem. Res.,* 2016, **4**:153
[9]. Farahmandjou M., Honarbakhsha S., Behrouziniab S. *Phys.Chem. Res.,* 2016, **4**:655
[10]. Agrawal D. *Mater Rese Innov.,* 2010, **14**:3
[11]. Hassan S., Gupta M. *Mater Sci Eng A.*, 2005, **39**:163
[12]. Jeyasimman D., Sivaprasad K., Sivasankaran S., Ponalagusamy R., Narayanasamy R., Iyer V. *Adv. Powder Technol*., 2015, **26**:139
[13]. Li J., Kwong F.L., Shi R.X., Ng D.H., Yin Y.S., *Mater Sci Eng A*., 2009, **52**:50
[14]. Mahapatra A., Mishra B.G., Hota G. *J Hazard Mater.,* 2013, **258**:116
[15]. Kim H.N., Lee S.K. *Am. Mineral,* 2013, **98**:1198
[16]. Wang J.A., Bokhimi X., Morales A., Novaro O.,Lo´pez T., Go´mez R. *J. Phys. Chem. B.,* 1999, **103**:299
[17]. Farahmandjou M., Honarbakhsh S., Behrouzinia S. *J. Supercond. Nov. Magn.*, 2018, **31**:4147
[18]. Farahmandjou M., Khalili P. *Aust. J. Basic Appl. Sci.*, 2013, **7**:462
[19]. Jurablu S., Farahmandjou M., Firoozabadi T.P. *J. Sci. Islamic Republic Iran*., 2015, **26**:281
[20]. Farahmandjou M., Dastpak M. *Phys. Chem. Res.*, 2018, **6**:713
[21]. Sohlberg K., Pennycook S.J., Pantelides S. T. *J. Am. Chem. Soc.*, 1999, **121**:10999
[22]. Celik Y., Suvacı E., Flahaut E., Weibel A., Peigney A. *J. Am. Ceram. Soc.,* 2010, **93:**3732
[23]. Yang Y., Wei H., Zhang L., Kisslinger K., Melcher C.L., Wu Y. *J. Lumin.,* 2015, **168**:297
[24]. Mokoena T.P., Linganiso E.C., Swart H.C., Kumar V., Ntwaeaborwa O.M. *Ceram. Int*., 2017, **43**:174
[25]. Kumar S., Prakash R., Kumar V., *Functional Materials Letters*, 2015, **8**:1550061
[26]. Rani G., Sahare P.D. *Adv. Powder Technol.*, 2014, **25**:767
[27]. Zhu Z., Liu D., Liu H., Wang X., Fu L., Wang D. *Ceram. Int.*, 2012, **38**:4137
[28]. Monteiro T., Boemare C., Soares M.J., Alves E., Marques C., McHargue C., Ononye L.C. Allard L.F. *Nucl. Instr. Meth. Phys. Res. B,* 2002, **191**:638
[29]. Alhaj Sakur A., Okdeh M., Al Fare B. *Mod Chem appl*., 2016, **4**:1
[30]. Heiba Z.K., Mohamed M.B., Wahba A.M., Imam N.G. *J. Electron. Mater.,* 2018, **47**:711
[31]. Khodadadi A., Farahmandjou M., Yaghoubi M., Amani A.R. *Int. J. Appl. Ceram. Technol.*, 2019, **16**:718
[32]. Dmitry Smovzh V., Salavat Sakhapov Z., Alexey Zaikovskii V., Sergey Novopashin A. *Ceram. Int*., 2015, **41**:8814
[33]. Farahmandjou M. *Revista Mexicana de Fisica*, 2013, **59**:205
[34]. Mora´n-Pineda M., Castillo S., Lo´pez T., Go´mez R., Cordero-Borboa A.E., Novaro O., *Appl. Catal.* B, 1999, **21**:79
[35]. Farahmandjou M., Golabiyan N. *Nano Micro Scales,* 2015, **3**:100
[36]. Farahmandjou M., Golabiyan N. *Ceramic Proc. Res.*, 2015, **16**:237
[37]. Janitabar Darzi S., Mohseni N. *Advanced Journal of Chemistry-Section A*, 2019, **2**:165
[38]. Janitabar Darzi S., Bastami H. *Advanced Journal of Chemistry-Section A,* 2021, DOI: 10.22034/ajca.2022.305643.1281
[39]. Scherrer P. *Gottingen. Mathematisch Physikalische Klasse*.,1918, **2**:98
[40]. Hafshejani L.D., S., Koponen H., Riikonen J.,Karhunen T., Tapper U., Lehto V.P., Moazed H., Naseri A., Hooshmand A., Jokiniemi J., Bhatnagar A.,Lähde A. *Powder Technol.,* 2016, **298**:42
[41]. Marami M.B., Farahmandjou M. *J. Electron. Mater.,* 2019, **48**:4740
[42]. Behrouzinia S., Salehinia D., Khorasani K., Farahmandjou M. *Opt. Commun.,* 2019, **436**:143

[43]. Farahmandjou M., Motaghi S. *Opt. Commun.,* 2019, **441**:1
[44]. Khodadadi A., Farahmandjou M., Yaghoubi M. *Mater. Res. Express.,* 2019, **6**:025029
[45]. Farahmandjou M., Salehizadeh S.A. *Glas. Phys. Chem,* 2013, **39**:473
[46]. Khatoon S., Wani I.A., Ahmed J., Magdaleno T., Al-Hartomy O.A., Ahmad T. *Mater. Chem. Phys.*, 2013, **138**:519
[47]. Kumar S., Kumar R., Singh D.P. *Appl. Surf. Sci.*, 2009, **255**:8014
[48]. Nomura K., Kinoshita R., Sakamoto I., Okabayashi J., Yamada Y. *Hyperfine Interact.*, 2012, **208**:65
[49]. Maldonado C.S., Rosa J.R., Lucio-Ortiz C.J., Hernández-Ramírez A., Barraza F.C., Valente J.S. *Materials*., 2014, **7**:2062

How to cite this manuscript: Abolfazl Khodadadi*, Mohammad Rahim Talebtash *. Investigation and synthesis of Fe doped Al_2O_3 nanoparticles by Co-precipitation and sol gel methods. *Asian Journal of Nanoscience and Materials*, 5(1) 2022, 36-47. DOI: 10.26655/AJNANOMAT.2022.1.4